INDIAN JOURNAL OF SCIENCE AND TECHNOLOGY

RESEARCH ARTICLE

A Study on Structural and Textural Feature Extraction for Contactless Fingerprint Classification

K C Deepika[1]*, **G Shivakumar**[2]

1 Assistant Professor, Department of E&C, Malnad College of Engineering, Hassan, Karnataka, India
2 Professor, Department of E&I, Malnad College of Engineering, Hassan, Karnataka, India

OPEN ACCESS

Received: 19-08-2022
Accepted: 29-09-2022
Published: 30-11-2022

Citation: Deepika KC, Shivakumar G (2022) A Study on Structural and Textural Feature Extraction for Contactless Fingerprint Classification. Indian Journal of Science and Technology 15(44): 2375-2385. https://doi.org/10.17485/IJST/v15i44.1471

* **Corresponding author**.

kcd@mcehassan.ac.in

Funding: None

Competing Interests: None

Published By Indian Society for Education and Environment (iSee)

ISSN
Print: 0974-6846
Electronic: 0974-5645

Abstract

Objectives: The Recent COVID 19 Pandemic has capped the efficacy of the mostly used existing touch-based fingerprint detection. Hence, the main objective of this study is to develop a lightweight, robust and efficient touchless fingerprint identification model. To cope up with touchless environment demands, an emphasis is made on improvement in local conditions, feature modalities as well as learning environment. **Methods:** Considering these objectives, the focus of this study is on two different methods for classification of contactless fingerprint. In the first method structural features like minutiae details are extracted followed by classification by SSIM. In the second method GLCM textural features were extracted followed by classification using Random Forest algorithm. In the proposed method, performance assessment is done by considering data samples of 1000 random users that are collected from different benchmark databases like Hong Kong Polytechnic University 3D-fngerprint images Database Version 2.0, Touchless Fingerprint Database of IIT Bombay, IIT Kanpur, IIT Jodhpur. **Findings:** Though, touchless fingerprint detection is considered as a viable alternative; yet, the real-time data complexities like non-linear textural patterns, dusts, non-uniform local conditions like illumination, contrast, orientation make it complex for realization. Moreover, the likelihood of ridge discontinuity and texture damages can majorly limit its efficacy. **Novelty:** The proposed model mainly focusses on reducing Equal Error Rate and improving the accuracy of contactless fingerprint classification by extracting textural features rather just sticking to conventional structural feature-minutiae. The Proposed method outperforms when compared with the existing state of the art methods by achieving an accuracy of 94.72%, precision of 98.84%, recall of 97.716%, F-Measure 0.9827 and a reduced EER of about 0.084. The key novelty of this approach was that it doesn't require any surface 3D reconstruction, rather it employed different mathematical approaches to retrieve surface normal and minutiae information.

Keywords: SSIM; GLCM; Contactless Fingerprint; Minutiae; EER; Confusion Matrix

1 Introduction

The last few decades have witnessed exponential rise in advanced technologies. Despite significant innovation and technological horizon, personalized security often remains a challenge under dynamic application environment. Unlike cryptographic concepts, in the last few years biometric driven authentication systems have increased significantly[1] having superior potential with high scalability, interoperability and time-efficiency. Its efficacy can easily be visualized as Aadhar Card system by Unique Identification Authority of India. Interestingly, more than a billion of population in India possesses a fingerprint driven Aadhar card for its verification. Though, Aadhar is a multi-modal system; however, evolved with fingerprint identification. In sync with such significances, a large number of efforts have been made by academia-industries; however, the recent pandemic of COVID-19[2] has limited the scope of the classical touch-based fingerprint authentication systems[3]. COVID-19 pandemic has almost limited the efficacy of the touch-based two-dimensional fingerprint driven modalities[4], as this pandemic was found exponentially spreading due to inter-personal infection through such frequently touching devices[5].

Considering above stated issues and scopes[6] in this research two techniques have been proposed first, extracting conventional structural feature say minutiae followed by classification by Structural Similarity Index Matching. Second, to cope up with touchless fingerprint identification system demands[7], in this paper, the emphasis was made on multi-dimensional optimization including pre-processing, feature extraction and eventual learning model[8]. Being touchless approach, we considered normal three-dimensional RGB images as input, which is then processed for histogram equalization followed by contrast improvement and filtering. Recalling, non-linear ridge value patterns and local textural variations, we performed image normalization using Z-score method. Here, we performed block-wise normalization to improve contrast information. Subsequently, orientation image estimation was performed to improve local feature distribution[9]. Moreover, it enabled frequency image estimation to make further feature learning better. As post frequency image estimation, we performed ridge mask generation and Gabor filtering to ensure optimal local spatial-temporal textural feature (STTF) distribution for further minutiae detection[10]. Finally, cropping the improved ridge mapping information, we performed STTF feature extraction by applying Gray-level Co-occurrence Matrix (GLCM). where his method helped in obtaining multi-dimensional textural features later applied random forest algorithm for fingerprint classification. The key novelty of this approach was that it is not depended only on conventional minutiae feature extraction rather shifted to improved multi-dimensional textural features and it doesn't require any surface reconstruction where many of the authors in literature survey have opted 3D reconstruction, rather it employed different mathematical approaches to retrieve surface normal and minutiae information.

Finally, assessment of both the proposed methods is carried out by obtaining Confusion Matrix for both the methods and concluded that textural features help in improving the efficacy of the classification of contactless 3D fingerprint classification. Also, the proposed method has reduced Equal Error Rate when compared with existing state of the art methods.

2 Methodology

This section primarily discusses the overall proposed contactless fingerprint detection and classification system. Unlike classical fingerprint detection models, in this research the focus is made on improving input data environment as well as feature vectors to

ensure highly accurate and reliable fingerprint detection and classification. Moreover, we intend to guarantee textural feature driven optimal feature extraction without depending on the classical minutiae detection and segmentation. To achieve it, the proposed work encompasses few tasks as depicted in Figure 1.

2.1 Data Acquisition

In sync with the targeted contactless environment for fingerprint detection system, in this work we collected contactless three-dimensional sensor driven images to prepare datasets. The 3D contactless fingerprint datasets were collected in such a manner that it could enable effective learning under data heterogeneity and diversity to make it more efficient under realistic environment. We considered the 3D Fingerprint dataset comprising a large contactless fingerprint sample. Noticeably, for our case study we considered a total of 50 subjects and the samples collected were from the subjects aged in between 28 to 55 years. The subjects comprised a total of 40 man and 10 women that eventually contributed 160 and 40 fingerprint samples, correspondingly. The data considered had been collected under natural light conditions with standard illumination. Here, no specific light or illumination control measure was applied. Also, for comparison with the state-of-the-art methods, In the proposed method, data samples from 1000 random users are collected from different benchmark databases (Hong Kong Polytechnic University 3D-fngerprint images Database Version 2.0, IIT Bombay, IIT Kanpur, Touchless Fingerprint Database, UNFIT database from Image Analysis and Biometrics Lab. IIT Jodhpur) are considered.

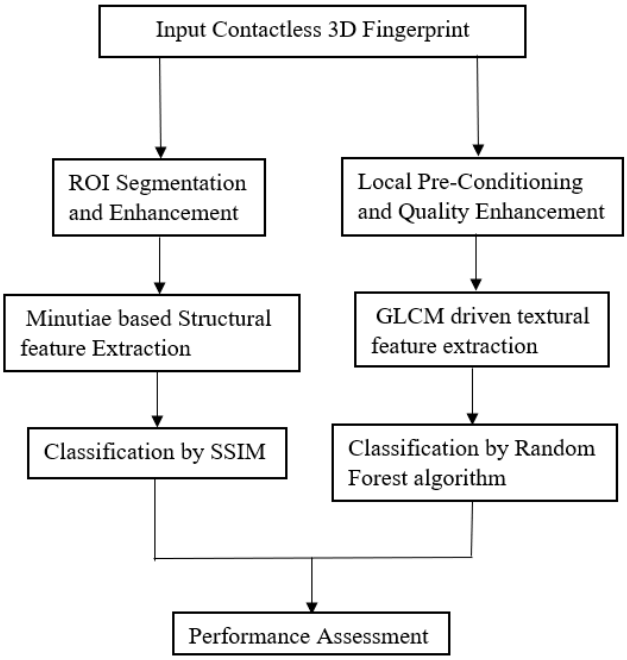

Fig 1. Proposed contactless fingerprint detection and classification model

2.2 Structural feature driven fingerprint classification

As already stated, realizing practical Touchless input acquisition and allied complexities, we processed each input sample for pre-processing. To achieve it, at first the input images were processed for image resizing. In this method, firstly the centroid of the fingerprint image was spotted using region –property function. With spotted centroid as a reference a radius of 120 pixels is marked and a circular ROI was estimated for each image. Once getting the ROI, it was handled for RGB to GRAY transformation. Over Gray output, histogram equalization was performed that alleviates major key problem of intensity variation over the retrieved images and makes it suitable for further processing. Later we have performed normalization followed by binarization. After obtaining the binary image of the fingerprint, we have performed thinning function that enabled skeleton formation of the image.

Above mentioned pre-processing tasks helps in extracting most of the ridge and structural information to achieve better accuracy. This process also helps in redundant data elimination that results in improvement in efficiency. The detailed discussion of the proposed minutiae estimation model is given in the sub-sequent section.

2.2.1 Minutiae Extraction

Typically, a justifiable illustration of a fingerprint can be provided in terms of its corresponding minutiae details. Among the all-possible minutiae details the ridge endings and bifurcations are the dominant one. Usually, ridge endings signify the points where the ridge curve stops or terminates, while bifurcations signify the specific location where a ridge splits from a single path into two paths at certain Y-type junction. To extract minutiae, we applied a simple Crossing-Number concept. In our applied crossing number concept, the binary image where the ridge flow pattern is eight-connected is considered. Now, performing scanning of the local neighborhood of each detected ridge pixel in the binary image with a 3×3 window, we extracted the minutiae in each fingerprint image. It has been followed by the estimation of crossing number value estimation, which is defined as half the sum of the differences between pairs of adjacent pixels in the eight neighborhoods. Subsequently, the ridge pixel has been classified as a ridge ending, bifurcation or non-minutiae point with the help of crossing-number properties. In this method, we have examined the local neighborhood of each ridge pixel with the help of a $3x3$ window that eventually yield extracted ridge endings and bifurcations from the skeleton image. To obtain the crossing number of a pixel P can be depicted as (1).

$$N_{Cross} = \frac{1}{2}\sum_{i=1}^{8}(P_i - P_{i+1}| \tag{1}$$

In above equation, the variable P_i states the binary pixel value in the neighborhood of P where $P_i = (0\ or\ 1)$ and $P_9 = P_1$. In this case for a pixel P, eight neighbouring pixels are scanned in anti-clockwise direction. Now with the corresponding values of the pixels and its crossing number values each pixel is categorized. Obtaining the thinned ridge map, we identified the ridge pixels with three ridge pixel neighbors, also called the ridge bifurcations. Thus, with one ridge pixel neighbor are stated to be the ridge endings. The absolute location (x,y) and the orientation (θ) are stored for each extracted minutia and thus the location of the minutiae is represented in terms of the distance from the core, while the core signifies coordinate $(0,0)$ on an x,y-axis. At the ridge-termination, the orientation or angle formed in between the horizontal line and core gives ridge angle. Thus, these obtained minutiae details can be used for comparison for fingerprint identification. Once obtaining the minutiae details, it has been processed for template matching using SSIM.

2.2.2 SSIM Based Minutiae Template Matching

SSIM is one of the most used image analysis tools used for quality assessment and image-matching purposes. It exhibits the similarity of the two distinct images based on certain features such as structural distortions, textural features, luminance etc. It performs image comparison not based on the pixel values rather the image elements identified by human. SSIM embodies varied distortions, including contrast, luminance and texture to compare fingerprint images. Noticeably, in our case, we applied minutiae details as the feature in SSIM to match fingerprint images of the users to make identification decision. The suitable values of SSIM can be in the range of -1 (maximum difference) to 1 (no difference). For our considered fingerprint minutiae picture, SSIM at coordinate (x,y) has been obtained using following mathematical model.

$$SSIM\,(x,y) = (l\,(x,y)]^{\alpha} \bullet (c\,(x,y)]^{\beta} \bullet (s\,(x,y)]^{\gamma} \tag{2}$$

$$l\,(x,y) = \frac{2\mu_x\mu_y + C_1}{\mu_x^2 + \mu_y^2 + C_1^{'}} \tag{3}$$

$$c\,(x,y) = \frac{2\sigma_x\sigma_y + C_2}{\sigma_x^2 + \sigma_y^2 + C_2^{'}} \tag{4}$$

$$s\,(x,y) = \frac{\sigma_{xy} + C_s}{\sigma_x\sigma_y + C_s^{'}} \tag{5}$$

$$C_s = \frac{c_2}{2} \tag{6}$$

and when $\alpha = \beta = \gamma = 1$ then

$$SSIM(x,y) = \frac{(2\mu_x\mu_y + C_1)(2\sigma_x + C_2)}{(\mu_x^2 + \mu_y^2 + C_1)(\sigma_x^2 + \sigma_y^2 + C_2)} \tag{7}$$

$$SSIM_{ij} = W_Y \bullet SSIM_{ij}^{Y} + W_{cb} \bullet SSIM_{ij}^{cb} + W_{cr} \bullet SSIM_{ij}^{cr} \tag{8}$$

The definitions of the different parameters applied in above equation are given as follows:

α, β, γ – Significance coefficients
μ_x – Average of the luminance sample for input minutiae signal x
μ_y- Average of the luminance sample for test signal y
σ_x - Deviation of the luminance sample for input minutiae signal x
σ_y - Deviation of the luminance sample for test signal y
σ_{xy} - Covariance of the luminance samples of two images x and y
C_1, C_2 – stabilizing factors or constants
W_Y – the weight value of Y
W_{cb}- the weight value of C_b
W_{cr} - the weight value of C_r

Thus, obtaining the value of (8), the two images can be same only when it has the SSIM value of 1. On contrary, low SSIM value signifies the disparity between fingerprint images or unmatched fingerprint.

2.3 GLCM Textural Features driven Fingerprint Classification

Let, I be the input fingerprint image with $N \times N$ dimensional matrix, with $I(i,j)$ as the pixel intensity for the ith row and the jth column. In sync with touchless input, we hypothesize that the input images possess minimum resolution of 600 dots per inch, which is not difficult in contemporary high-definition camera. Thus, for the input images with aforesaid specification, the mean and the variance of the fingerprint image I in its gray-level form are derived as equation (9) and (10) respectively.

$$M(I) = \frac{1}{N^2} \sum_{i=0}^{N-1} \sum_{j=0}^{N-1} I(i,j) \tag{9}$$

$$Var(I) = \frac{1}{N^2} \sum_{i=0}^{N-1} \sum_{j=0}^{N-1} (I(i,j) - M(I))^2 \tag{10}$$

Consider that the orientation image be O, with the dimension $N \times N$. Moreover, $O(i,j)$ be the local ridge representation at the pixel instant (i,j). Noticeably, over touchless multi-dimensional image, the local ridge orientation can be characterized for a block in comparison to each pixel-based analysis. In this reference, an input fingerprint image can be split into multiple non-overlapping blocks ($w \times w$), where each local ridge orientation is obtained for each block. Noticeably, in case of a typical fingerprint image the local ridge orientation at 900 and 2700 remains to be the same and can't be distinguished. This is mainly because the ridge oriented at both 900 and 2700 remains the same. Similarly, over a frequency image (F), which is defined with $N \times N$ dimensional image, let $F(i,j)$ be the local ridge frequency. Here, local ridge frequency refers the frequency of the ridge and furrow structure in adjacency, especially in orthogonal to the local ridge orientation. To be noted, the ridge and furrow structure in adjacency often shows a feature where minutiae doesn't constitute any specific and well-structured sinusoidal-shaped wave. In this case, the frequency is characterized as the mean frequency of its neighbors. Similar to the orientation image, frequency image is also characterized in block-wise manner. The proposed model also applies region-masking concept, which is also performed over each block sequentially to improve intrinsic features per image so as to improve better feature extraction and learning over touchless fingerprint images. Here, we define region masking, R as a $N \times N$ image, possessing $R(i,j)$ signifying the type of the pixel. Thus, each pixel can be classified into two broad categories; first, non-recoverable ridge-and-furrow pixel and second, recoverable ridge-and-furrow pixels, which are labelled as 0 and 1, respectively.

In this proposed work, GLCM functions as a descriptive statistical feature distribution model assessing the probability of the pixel's gray scale values over an input fingerprint image. Functionally, it extracts high-dimensional statistical features.

In this work, we assume that after preprocessing, the varied textural features are distributed uniformly throughout the pre-processed input image. In this reference, over each input fingerprint image we extracted the different textural features, which were later combined together to yield a composite feature vector for classification. In this method, the retrieved textural features were derived in the form of a matrix representing pixel intensities $I(x,y)$, centered on the pixels (x,y). In this manner, we extracted different textural features for each input touchless pre-processed images, with distinct probability matrix $P_{i,j}$. Here, the above stated probability matrix signifies the differences of the intensity between the pixel elements i and j that later helps in detecting motion patterns. In GLCM gray-scale refers the pair association along a direction, and therefore retrieving the gray-scale values can yield a matrix representing the association matrix among the pixels towards the target direction. We obtained symmetric matrix S by amalgamating the gray-scale information along with the allied transpose values. It enables estimation of the cumulative relationship among the pixels in one direction. We normalized the association matrix S using (11) to obtain the probability matrix $P_{i,j}$.

$$P_{i,j} = \frac{S_{i,j}}{\sum_{i,j=0}^{N-1} S_{i,j}} \tag{11}$$

With the extracted values of $P_{i,j}$, the different textural features including the following were obtained.

- Contrast,
- Energy,
- Homogeneity,
- Correlation,
- Mean,
- Standard deviation,
- Variance,
- Kurtosis, and
- Skewness.

As stated, a total of nine STTF features were obtained for further feature learning. Here, our predominant goal was to retain maximum possible and significant features for learning and classification so as to achieve higher accuracy. The brief of GLCM features extracted is discussed below:

2.3.1 ***Contrast***

In GLCM, contrast is defined as the variation in gray scale parameter values over the input image. With the derived probability matrix (11), the pixel pairs representing the diagonal element represents vital difference in contrast values. Here, the texture contrast represents the cumulative variations in the local pixel intensities across the input fingerprint image. Generally, the non-linearity existing across the input image is examined by performing statistical estimation and corresponding textural continuity assessment. We measured the contrast information for each input fingerprint image using equation (16).

2.3.2 ***Energy***

To examine energy distribution across the image, the proposed model measured angular second moment (ASM) value that measures the rotational acceleration over the input feature space. Here, the model defined in (12) was applied to estimate the ASM value. Typically, the value of ASM increases linearly throughout the gray-level values over input image.

$$ASM = \sum_{i,j=0}^{N-1} {P_{i,j}}^2 \tag{12}$$

Once calculating the ASM values (12), we estimated the energy parameter using (13).

$$ENR = \sqrt{ASM_{i,j}} \tag{13}$$

2.3.3 ***Entropy***

Entropy, which is also referred as the pixel-disturbances within an input image. In other words, it also signifies how non-linear the gray-level values are distributed throughput the input fingerprint image. Typically, the entropy value increases with rise in pixel's non-linear distribution. We applied (14) to estimate the entropy value.

$$ENT = \sum_{i,j=0}^{N-1} P_{i,j}\left(-lnP_{i,j}\right) \tag{14}$$

2.3.4 ***Homogeneity***

Typically, homogeneity refers the Inverse Different Moment (IDM) signifying higher homogeneity with reference to the lower contrast. In other words, an input image would have lower homogeneity with higher contrast. In this work, we used equation (15) to measure homogeneity distribution throughput the input fingerprint image.

$$HOM = \sum_{i,j=0}^{N-1} \frac{P_{i,j}}{1+(i-j)^2} \tag{15}$$

In reference to the linear magnitude distribution over input fingerprint image, smaller value of contrast would give rise to the higher homogeneity. In this work, we employed equation (16) to measure contrast over the input image.

$$CONT = \sum_{i,j=0}^{N-1} P_{i,j}(i-j)^2 \tag{16}$$

2.3.5 ***Correlation***

Correlation signifies the statistical feature representing descriptive statistics throughout the input image. In this work, in addition to the correlation information (16), we extracted three other spatial-temporal statistical features encompassing mean, standard deviation, and variance. In order to estimate the mean value, we employed the symmetric features of the probability matrix $P_{i,j}$ (11). Mathematically, we applied equations (17) and (18) to estimate the mean values for the different pixel instants.

$$\mu_i = \sum_{i,j}^{N-1} i\,(P_{i,j}) \tag{17}$$

$$\mu_j = \sum_{i,j}^{N-1} j\,(P_{i,j}) \tag{18}$$

Further, we applied mean values (17-18), variance and standard deviation values were obtained by applying equations (19) and (20), respectively.

$$\sigma_i^2 = \sum_{i,j}^{N-1} P_{i,j}(i-\mu_i)^2 \tag{19}$$

$$\sigma_i = \sqrt{\sigma_i^2}$$

$$\sigma_j = \sqrt{\sigma_j^2} \tag{20}$$

Thus, estimating the mean and variance values, we estimated correlation information using (21).

$$CORR = \sum_{i,j}^{N-1} P_{i,j} \left[\frac{(i-\mu_i)\,(j-\mu_j)}{\sqrt{\left(\sigma_i^2\right)\left(\sigma_j^2\right)}} \right] \tag{21}$$

2.3.5 ***Skewness***

With the above stated statistical features, we extracted directional or orientational features, including skewness and Kurtosis. These features are also called as the symmetrical statistical features. With the estimated probability matrix (11), skewness parameter refers the lack of symmetry. In case of at image processing tasks, skewness is defined in the form of shade feature where the high cluster-shade signifies asymmetrical nature. We applied equation (22) to estimate the skewness values per input fingerprint image.

$$SKEW = \sum_{i,j}^{N-1} P_{i,j}(i-\mu_i+j-\mu_j)^4 \tag{22}$$

2.3.7 ***Kurtosis***

Kurtosis signifies strength of the input gray-level values distributed throughput the input fingerprint image. Here, higher Kurtosis confirms or indicates that the amount of the feature-distribution is mainly strenuous along tail than the mean value. The lower value of Kurtosis indicates that the amount of feature-distribution remains strenuous in the direction of the spike which is closer to the mean value. In this work, Kurtosis was obtained over the entire input image as there is no specific target area and throughout image serves as an input textural feature to make learning and further classification. Once extracting above stated nine different GLCM features, we performed horizontal concatenation to estimate a composite feature vector for further learning. The composite GLCM feature obtained is given in equation (23).

$$GLCM_{Feat} = Conc(CONT,\ ENE, HOM, CORR, Mean,\ Var, STD, Kur, Skw) \tag{23}$$

Now, once estimating the composite feature vector (i.e., $GLCM_{Feat}$), we projected it for feature learning and classification by Random Forest algorithm.

2.3.8 ***Random Forest Algorithm***

Random Forest is one of the most successful learning algorithms that structurally encompasses multiple tree-based classifiers, behaving as an ensemble learning model. In the proposed tree-model, each tree provides its corresponding vote for the most probable class for each input fingerprint image. Let the total training samples be N, then a sample encompassing N cases are randomly selected from the original data. These selected samples are further employed as training set to form a new tree. Now, in case there are M input variables, then the best split on these M is applied to split the node. Here, we maintained the value of M as constant during forest development, also called as the growing phase. In this manner, each tree is developed to the largest extent. Unlike classical machine learning methods, Random Forest algorithm needs smaller number of parameters to be estimated during classification. It makes overall computation more efficient and suitable for the real-time uses. A complete Random Forest algorithm can be eventually defined as the combination of the different tree-structures, as presented in (24).

$$(h(x, \theta_k)\ ,\ (k = 1, 2, \ldots i \ldots\} \tag{24}$$

In (24), the parameter h signifies the classifier function, while $(\theta_k\}$ presents the random vector distributed identical. Here, each tree contains a vote for the most probable class for a specific SQL query as input x. The dimensionality of θ primarily depends on its use in the tree formation. In fact, the key reason behind random forest success is its ability towards the formation of each decision tree which forms the forest. In the proposed method, we used a bootstrapped subset of training samples to train each tree throughout the constructed forest that enables almost 70% of the training data usages, while the remaining dataset is labelled as the out-of-bag samples that is later used to perform inner cross-validation to examine the classification results and enhance it. Thus, applying this ensemble learning method, we performed fingerprint classification for the different input samples.

3 Results and Discussion

Considering the significance of a touchless 3D fingerprint identification and classification system, in this research as a first method a minutiae-based measure was proposed where we focused on at first setting up an optimal data environment, followed by feature extraction mechanism and pattern matching followed by classification. Understanding the way that the touchless data acquisition might undergo different local environmental changes such as change in brightness, contrast and skin defects an efficient pre-processing was carried out and the results of preprocessing are shown in Figure 2. Realizing the fact that in majority of the 2D as well as 3D fingerprint identification methods, authors have applied Minutiae features and template matching, we at first applied crossing number-based minutiae extraction and matching to label input fingerprint as 1 and 0, signifying Identified and Unidentified correspondingly. To examine the performance of the proposed model, we have obtained confusion matrix. Eventually to characterize performance we have obtained different statistical components like Accuracy, Precision, F-Measure, and Recall. Results are listed and compared in Figure 4.

Now, we mainly focus on assessing efficacy of the proposed textural feature driven contactless fingerprint detection and classification model, qualitatively as well as quantitatively. In other words, here we examine whether the use of local pre-conditioned image improvement yields superior performance. Before discussing the simulation results quantitatively, a snippet of pre-conditioned and enhanced results is shown in Figure 3. Figure 3 (a) presents a random input 3D touchless fingerprint image. Here, it can easily be visualized that the illumination at the image center and bottom is relatively higher in comparison to the top corners. Moreover, the ridge structures in lower right bottom are unclear with high level of ambiguity. Furthermore, the straight division lines on the left side (bottom to top) can easily be visualized in this sample image, which can disrupt the

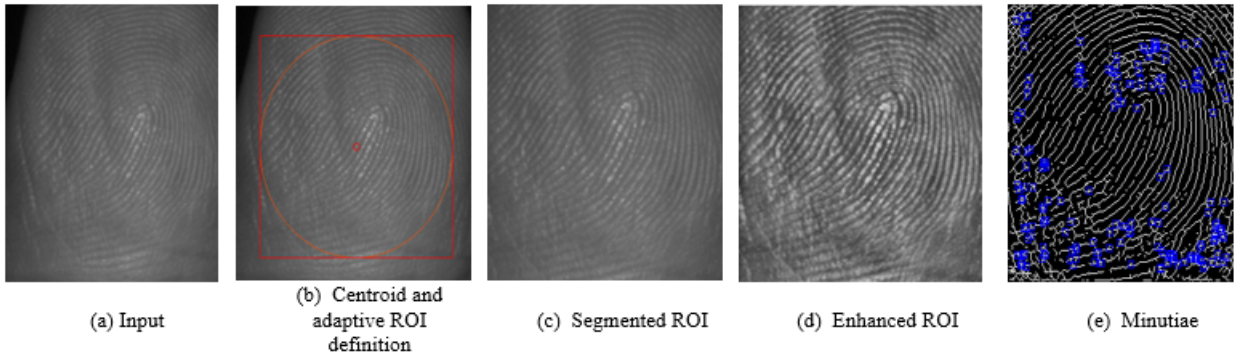

Fig 2. Preprocessed results and extracted structural feature

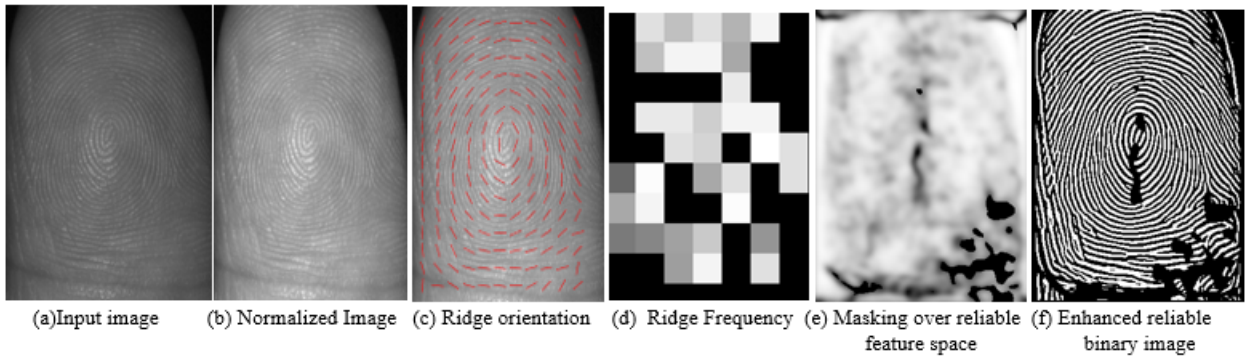

Fig 3. Locally improvedfingerprint images for textural feature extraction

ridge continuity to make further cue-segmentation or allied feature learning. Noticeably, there are numerous use environment where due to local conditions such as low temperature, salty water contact etc. the ridge values get changed temporarily. Though, with touch-based classical methods while pressing finger over the sensor such local deformations get suppressed; however, in touchless fingerprint detection it can have decisive impact on feature learning and hence classification. To alleviate such issues, we performed local pre-conditioning driven pre-processing to improve the image quality for further feature extraction. As repeatedly stated in the previous sections, we intended to guarantee ridge continuity over the different local conditions while ensuring that the ridges contain sufficient intrinsic features. To achieve it, we applied the different pre-processing steps like image normalization, ridge orientation estimation, frequency estimation, ridge mapping and filtering. Figure 3 (b) presents the normalized image output obtained from the original input image. Here, the impact of normalization can easily be visualized. Now, recalling the methodological intend where we intended to improve ridge structure continuity even over non-linear textural fingerprint surfaces, we performed ridge orientation estimation Figure 3 (c). The ridge frequency obtained over each grid is given in Figure 3 (d). Figure 3 (e) presents the ridge masking results where the high frequent ridges are masked as 1, while the less frequent ridges are labelled as 0. Here, the key motive was to retain the ridge information carrying densely distributed features. Here, observing the results it can easily be understood that the improved 3D touchless fingerprint image caries more uniform ridge's distribution with precisely perceptible structure, which can provide more efficient feature vectors for further learning and classification. To characterize performance, we have obtained different statistical components like Accuracy, Precision, F-Measure, and Recall as listed and compared in Figure 4.

This is the matter of fact that a large number of studies have been done towards touch-based fingerprint detection systems; however, the efforts made towards touchless fingerprint detection are countable and very rare. Our depth literature assessment revealed that merely countable a dozen of efforts is made so far to introduce 3D touchless data for fingerprint detection. To assess relative performance, we have selected the couple of recent methods listed in Table 1. The comparison of Equal Error rate of existing methods and the proposed method is shown in Table 1. The key novelty and advantage of this approach is that it don't require any surface reconstruction, rather it employed different mathematical approaches to retrieve surface normal and minutiae information. Which was later used for learning and classification. Thus, observing performance outcomes and allied

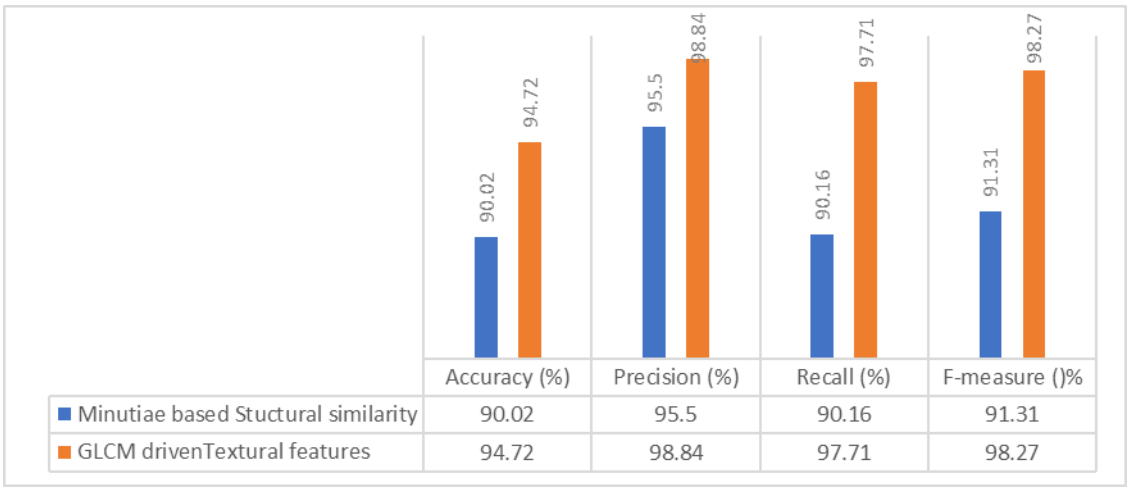

Fig 4. Performance comparison of structural and textural features driven classification

Table 1. Comparison of Equal error rate of the proposed method with the existing state of the art methods

Paper	Method Implemented	Database used	Features extracted	Assessment of EER in %
X. Yin, Y. Zhu, and J. Hu [11]	3D Reconstruction	3D Stereo images	TTP features	0.66
J. Galbally. L. Beslay G. Böstrom [12]	Deep CNN	3D-FLARE DB	HOG+LBP	1.04
Bakheet, S, Alsubai, S, Alqahtani, A, Binbusayyis [13]	SIFT	FVC2004	Minutiae	2.01
Priesnitz, J, Huesmann, R, Rathgeb C, Buchmann N, Busch [14]	VeriFinger	PolyU	Minutiae	3.17
Attrish A, Bharat N, Anand V, Kanhangad V [15]	Deep CNN	IITI-CFD	Minutiae	2.19
Birajadar P, Haria M, Kulkarni P [16]	VeriFinger	IITB	Minutiae	1.18
Proposed Method	GLCM + RF	PolyU+ IITB	Textural Features	**0.084**

inferences, it can be stated that the proposed touchless fingerprint detection model outperforms other state-of-art methods by achieving a reduced EER of 0.084.

4 Conclusion

The fingerprint detection models have always been considered as a vital alternative of the classical cryptosystems. Undeniably, being fast in execution fingerprint-based systems turn out to be more efficient solution for personalized security. This efficacy makes fingerprint-based authentication system as one of the most used approaches. Despite robustness, being touch-based paradigm, its optimality has challenges under different operating environment, especially in reference to the health and hygiene. During the recent pandemic of COVID-19, touch-based fingerprint models were found vulnerable due to touch-based infection probability. To alleviate such issues, contactless fingerprint detection method can be a viable solution; however, being touchless in nature such approaches might undergo different complexities like the impact of viewing angle, textural non-linearity, non-uniform illumination and contrast, ridge and furrow ambiguity, ridge discontinuity etc. Extracting conventional structural features like minutiae over aforesaid local adversaries can impact overall efficacy. On the other hand, to cope up with touchless environment demands, an improvement in local conditions and feature modalities followed by training over textural features improves accuracy and also minimizes EER. Quantitatively the Proposed method outperforms when compared with the existing state of the art methods on the benchmark database by achieving an accuracy of 94.72%, precision of 98.84%, recall of 97.716%, F-Measure 0.9827 and a reduced EER of about 0.084. The key novelty of this approach was that it didn't require any surface reconstruction, rather it employed different mathematical approaches to retrieve surface normal and minutiae information.

As a future work we can experiment with the different feature extraction methods like CNN or hybrid techniques also we can experiment with ensemble learning algorithms to still improve the accuracy of classification.

5 Acknowledgement

The Authors would like to thank the management, Principal and authorities of Malnad College of Engineering, Hassan for extending full support in carrying out this research work.

References

1) Thakor VA, Razzaque MA, Khandaker MRA. Lightweight Cryptography Algorithms for Resource-Constrained IoT Devices: A Review, Comparison and Research Opportunities. *IEEE Access*. 2021;9:28177–28193. Available from: https://doi:10.1109/ACCESS.2021.3052867.
2) N, V S, Vendhan A, M. Rejuvenation of online research interactive fora during COVID-19. *Indian Journal of Science and Technology*. 2020;13(47):4603–4605. Available from: https://doi:10.17485/IJST/v13i47.2230.
3) Wild P, Daubner F, Penz H, Dominguez GF. Comparative Test of Smartphone Finger Photo vs. Touch-based Cross-sensor Fingerprint Recognition. *2019 7th International Workshop on Biometrics and Forensics (IWBF)*. 2019;p. 1–6. Available from: https://doi:10.1109/IWBF.2019.8739191.
4) Deepika KC, Shivakumar G. Towards More Accurate Touchless Fingerprint Classification Using Deep Learning and SVM. Data Science and Computational Intelligence. *International Conference on Information Processing, Data Science and Computational Intelligence pp*. 2021;p. 248–257. Available from: https://doi.org/10.1007/978-3-030-91244-4_20.
5) Deepika KC, Shivakumar G. A Robust Deep Features Enabled Touchless 3D-Fingerprint Classification System. *SN Computer Science*. 2021;2(4):263. Available from: https://doi.org/10.1007/s42979-021-00657-x.
6) Sagiroglu S, Ulker M, Arslan B. Mobile Touchless Fingerprint Acquisition And Enhancement System. *2020 IEEE Congress on Evolutionary Computation (CEC)*. 2020;p. 1–8. Available from: https://doi:10.1109/CEC48606.2020.9185870.
7) Priesnitz J, Rathgeb C, Buchmann N, Busch C, Margraf M. An overview of touchless 2D fingerprint recognition. *EURASIP Journal on Image and Video Processing*. 2021;2021(1). Available from: https://doi.org/10.1186/s13640-021-00548-4.
8) Priesnitz J, Rathgeb C, Buchmann N, Busch C. Touchless Fingerprint Sample Quality: Prerequisites for the Applicability of NFIQ2.0. *International Conference of the Biometrics Special Interest Group (BIOSIG)*. 2020;p. 1–5.
9) Deepika KC, Shivakumar G. Local Pre-Conditioning and Quality Enhancement to Handle Different Data Complexities in Contactless Fingerprint Classification. *International Journal of Advanced Computer Science and Applications (IJACSA)*. 2022;13(8). Available from: https://doi:10.14569/IJACSA.2022.0130875.
10) Tan H, Kumar A. Towards More Accurate Contactless Fingerprint Minutiae Extraction and Pose-Invariant Matching. *IEEE Transactions on Information Forensics and Security*. 2020;15:1. Available from: https://doi:10.1109/TIFS.2020.3001732.
11) Yin X, Zhu Y, Hu J. 3D Fingerprint Recognition based on Ridge-Valley-Guided 3D Reconstruction and 3D Topology Polymer Feature Extraction. *IEEE Transactions on Pattern Analysis and Machine Intelligence*. 2021;43(3):1085–1091. Available from: https://doi:10.1109/TPAMI.2019.2949299.
12) Galbally J, Beslay L, Bostrom G. 3D-FLARE: A Touchless Full-3D Fingerprint Recognition System Based on Laser Sensing. *IEEE Access*. 2020;8:145513–145534. Available from: https://doi:10.1109/ACCESS.2020.3014796.
13) Bakheet S, Alsubai S, Alqahtani A, Binbusayyis A. Robust Fingerprint Minutiae Extraction and Matching Based on Improved SIFT Features. *Applied Sciences*. 2022;12(12):6122. Available from: https://doi.org/10.3390/app12126122.
14) Priesnitz J, Huesmann R, Rathgeb C, Buchmann N, Busch C. Mobile Contactless Fingerprint Recognition: Implementation, Performance and Usability Aspects. *Sensors*. 2022;22(3):792. Available from: https://doi.org/10.3390/s22030792.
15) Attrish A, Bharat N, Anand V, Kanhangad V. A Contactless Fingerprint Recognition System. . Available from: https://doi.org/10.48550/arXiv.2108.09048.
16) Birajadar P, Haria M, Kulkarni P, Gupta S, Joshi P, Singh B, et al. Towards smartphone-based touchless fingerprint recognition. *Sādhanā*. 2019;44(7):161. Available from: https://doi.org/10.1007/s12046-019-1138-5.